DOI: 10.1093/brain/awh069 *Brain* (2004), **127,** 591–601

Differential impact of the *FMR1* gene on visual processing in fragile X syndrome

Cary S. Kogan,[1] Isabelle Boutet,[1] Kim Cornish,[2] Shahin Zangenehpour,[1] Kathy T. Mullen,[3] Jeanette J. A. Holden,[6] Vazken M. Der Kaloustian,[4] Eva Andermann[5] and Avi Chaudhuri[1]

[1]*Department of Psychology,* [2]*Department of Educational Psychology and Neurology and Neurosurgery,* [3]*McGill Vision Research, Department of Ophthalmology,* [4]*Departments of Pediatrics and Human Genetics, McGill University* [5]*Departments of Neurology and Neurosurgery and Human Genetics, McGill University and the Montreal Neurological Hospital and Institute, Montreal, Québec and* [6]*Departments of Psychiatry and Physiology, Queen's University, Kingston, Ontario, Canada*

Correspondence to: Avi Chaudhuri Department of Psychology, McGill University, 1205 Dr Penfield Avenue, Montréal, Québec H3A 1B1, Canada.
E-mail: avi@psych.mcgill.ca

Summary

Fragile X syndrome (FXS) is the most common form of heritable mental retardation, affecting ~1 in 4000 males. The syndrome arises from expansion of a trinucleotide repeat in the 5′-untranslated region of the fragile X mental retardation 1 (*FMR1*) gene, leading to methylation of the promoter sequence and lack of the fragile X mental retardation protein (FMRP). Affected individuals display a unique neurobehavioural phenotype that includes striking visual-motor deficits. Here we provide neurobiological and behavioural evidence that supports the hypothesis that these visual-motor deficits are attributable to a magnocellular (M) visual pathway impairment. Immunohistochemical staining of a lateral geniculate nucleus (LGN) of a normal human male revealed high FMRP basal expression selectively within the M layers, suggesting an increased susceptibility of these neurons to the lack of FMRP as occurs in FXS. Similar staining of monkey LGNs for quantification purposes revealed that the difference is not an artefact of cell size differences between M and parvocellular (P) neurons. Further, Nissl staining of the LGNs of a male FXS patient revealed alaminar nuclei comprised of a homogenous population of small sized neurons, providing anatomical and morphological support for the idea that an M pathway pathology exists in FXS. Consistent with these neurobiological data, we have found that male patients with FXS have reduced sensitivity for psychophysical stimuli that probe the M pathway but not for those that probe the P pathway, a complementary visual stream that performs a separate set of early visual operations. Finally, male patients with FXS performed poorly on a global motion task but not on a form perception task, suggesting that the M pathway thalamic deficit may have a selective impact on cortical visual functioning in the parietal lobe, which is known to be a major recipient of M pathway afferents via the primary visual cortex. Together, these findings provide the first evidence that the loss of a single gene product, FMRP, in humans leads to abnormal neuroanatomical morphology of the LGN and a concomitant selective visual deficit of the M pathway.

Keywords: fragile X syndrome; psychophysics; histology; LGN; *FMR1*

Abbreviations: CA = chronological age; DS = dorsal stream; *FMR1* = fragile X mental retardation 1 gene; FMRP = fragile X mental retardation protein; FXS = fragile X syndrome; LGN = lateral geniculate nucleus; M = magnocellular; MA = verbal mental age; P = parvocellular; VS = ventral stream; PBS = phosphate-buffered saline

Received September 3, 2003. Revised October 25, 2003. Accepted October 25, 2003. Advanced Access publication January 21, 2004

Introduction

By virtue of its single gene aetiology, fragile X syndrome (FXS) represents a unique model for understanding the impact of one protein on brain development, function and behaviour. FXS is the most common form of heritable mental retardation, affecting ~1 in 4000 males (Turner *et al*., 1996). Unlike females affected by the mutation, full mutation males are hemizygous and therefore often display a more pronounced phenotype that is characterized by uneven abilities

within and across cognitive domains. The syndrome results from expansion of a trinucleotide (CGG) repeat in the 5′-untranslated region of the fragile X mental retardation 1 (*FMR1*) gene, leading to aberrant methylation of the promoter sequence and, in males, a lack of the fragile X mental retardation protein (FMRP) (Oberle *et al*., 1991; Pieretti *et al*., 1991; Verkerk *et al*., 1991).

Recent advances have better elucidated the role of FMRP in cellular events. FMRP regulates the translation of a subset of proteins important for synaptic development and plasticity (Comery *et al*., 1997; Irwin *et al*., 2000). By examining the visual cortices of knock-out mice lacking the *fmr1* gene as well as those of FXS patients, Greenough and colleagues have shown that FMRP is critical to the pruning and maturation of dendritic spines (Greenough *et al*., 2001; Irwin *et al*., 2001, 2002; Churchill *et al*., 2002). Neurons within the visual cortex lacking FMRP maintain characteristically immature dendritic spines that are similar to the morphology of neurons of animals deprived of sensory experience. Furthermore, in FXS patients, the density of immature spines was found to be elevated compared with that in normal control brains, suggesting a lack of appropriate synaptic elimination. The absence of FMRP may therefore lead to abnormal brain morphology and function. MRI studies of brain structure have shown significant decreases in the cerebellar vermis size as well as enlargement of the fourth ventricle in FXS patients (Mostofsky *et al*., 1998). A more recent MRI study of neuroanatomical differences in children and adolescents with FXS revealed significantly enlarged caudate nuclei and ventricular CSF volumes as well as modestly enlarged thalamic volumes (Eliez *et al*., 2001).

Recent research endeavours have provided a more detailed account of the neurobehavioural profile associated with FXS. Relative strengths are apparent in vocabulary (Dykens *et al*., 1989), long-term memory for meaningful and learned information (Freund and Reiss, 1991) and face emotion perception (Turk and Cornish, 1998). These strengths are accompanied by relative weaknesses in attentional control (Munir *et al*., 2000*b*; Cornish *et al*., 2001; Wilding *et al*., 2002), working memory (Schapiro *et al*., 1995; Jakala *et al*., 1997; Munir *et al*., 2000*a*), linguistic processing (Belser and Sudhalter, 2001) and visual spatial cognition (Cornish *et al*., 1998, 1999). The pattern and severity of this profile serve to distinguish FXS from other forms of mental retardation. At a behavioural level, findings indicate three core deficits, namely impulsivity, hyper-arousal and anxiety (Turk, 1998; Hagerman and Hagerman, 2002). The associated difficulties in maintaining attentional skills and freedom from distractibility contribute to the apparently high rate of attention deficit disorders in males with FXS (Hagerman, 1987). Social and communication deficits also follow a characteristic profile, with many affected males displaying autistic-like features (Reiss and Freund, 1990). A striking aspect of the FXS neurobehavioural phenotype is impaired performance on neuropsychological tasks that assess visual-motor function. Visual-motor impairments have been described for tasks that require drawing skills (e.g. Crowe and Hay, 1990; Freund and Reiss, 1991), tasks that involve manipulation of blocks to construct abstract designs (e.g. Crowe and Hay, 1990; Cornish *et al*., 1999) and tasks requiring psychomotor coordination, such as the pegboard (e.g. Cornish *et al*. 1999) (for a comprehensive review see Hagerman and Hagerman, 2002). Although these tasks are multifactorial in nature, with performance affected by many causes, visual-motor ability is a common feature. Therefore, we postulated that the visual-motor deficiencies observed in FXS may reflect underlying neuroanatomical and functional abnormalities specific to the thalamic component of one of the two main parallel visual pathways, the so-called magnocellular (M) pathway.

Visual information is analysed by two anatomically and functionally segregated streams, the dorsal (DS) and ventral (VS) visual stream (Ungerleider and Mishkin, 1982; Milner and Goodale, 1995; Felleman *et al*., 1997). Although there is mixing of low-level inputs from the thalamus at higher stages, the two streams largely draw on separate afferent inputs, starting from the retina and the lateral geniculate nucleus (LGN). The LGN, in both humans and non-human primates, is a subcortical structure that relays visual information from the retina to the primary visual cortex and has been described as serving a gating function. The DS is largely dependent on afferent input from the M pathway (Vidyasagar, 2001; Le *et al*., 2002) and is thought to be crucial in the visual control of action (Milner and Goodale, 1995). The M pathway is specialized for the analysis of temporally modulated stimuli, such as object motion. The VS, on the other hand, is relatively more dependent on afferent input from the parvocellular (P) pathway of the LGN and is thought to be involved in pattern recognition and object identity (Milner and Goodale, 1995). The characteristics of the P pathway are consistent with this function because of its well-characterized role in processing visual aspects related to image structure, such as form, texture and colour.

In the present study, we have conducted neurobiological and psychophysical experiments to evaluate the possibility of a selective M pathway and DS deficit in FXS. Immunohistochemical and histological staining of normal human and monkey LGN, as well as FXS human LGN were conducted to assess whether M neurons are more susceptible to the loss of FMRP as occurs in FXS. Further, to evaluate the possibility of a perceptual deficit resulting from neurobiological changes in FXS, we employed tasks that optimally recruit the M pathway and DS processing. To ensure that this impairment was not due to a general perceptual deficit, we also employed tasks that optimally recruit the P pathway and VS processing, brain areas that should not be affected by the loss of FMRP. Finding that M neurons express more FMRP than P neurons would suggest their greater reliance on the protein and would point to their increased vulnerability to FMRP loss. Direct human evidence demonstrating morphological changes to the M neurons of FXS patients would lend further support to the notion of a selective M pathway

impairment in FXS. Finally, combining the neurobiological data with evidence of a functional impact in the form of deficits for detection of stimuli normally processed by the M pathway would confirm our hypothesis of an M pathway pathology in FXS.

Methods

Immunohistochemistry

Two adult male vervet monkeys (*Cercopithicus aethiops*) were used in this study. Animals initially were anaesthetized with ketamine hydrochloride (10 mg/kg, i.m.), euthanized with an overdose of sodium pentobarbital (25 mg/kg, i.v.), and then perfused transcardially with 0.1 M phosphate-buffered saline (PBS) until completely exsanguinated. The externalized brain was blocked along the midline followed by a coronal block chosen so as to include the LGN, and then flash-frozen in a liquid nitrogen/isopentane bath. At a later date, sections were cut on a cryostat from the frozen blocks at a thickness of 20 μm and mounted on Vectabond® subbed slides (Vector Laboratories, Burlingame, CA).

Human tissue was obtained from the Brain and Tissue Bank for Developmental Disorders, University of Maryland, Maryland and comprised one male normal control LGN (left hemisphere) and two LGNs from a male FXS-affected individual (both hemispheres). These tissue blocks were paraffinized according to a standard protocol. Sections were then cut on a sliding microtome at a thickness of 10 μm, mounted on subbed slides, deparaffinized, and rehydrated. Antigen recovery was accomplished with the Antigen Unmasking Solution® (Vector Laboratories) according to the manufacturer's protocol prior to standard Nissl staining or FMRP immunohistochemistry.

For FMRP staining of monkey LGN, the mounted sections were fixed in 4% paraformaldehyde for 10 min, washed three times in 0.1 M PBS, incubated in 1% hydrogen peroxide in 0.1 M PBS for 20 min, incubated twice in a 0.05% acetic anhydride solution, and blocked in 3% normal horse serum in 0.1 M PBS for 30 min prior to an overnight incubation in the anti-FMRP antisera (1 : 5000; Chemicon International, Inc., Temecula, CA). For the human LGN, we employed the same protocol with the exception of post-fixation and acetic anhydride treatment. Both monkey and human tissue sections were then incubated for 2 h in biotinylated secondary antisera (1 : 500; anti-mouse raised in horse) in 3% normal horse serum in 0.1 M PBS. Sections were then washed three times in 0.1 M PBS and incubated for 1 h in avidin–biotin–peroxidase complex (Vector Laboratories). Peroxidase activity was labelled for 10 min with a 3,3-diaminobenzidine kit (Vector Laboratories).

For neuron-specific enolase staining of monkey LGN, the mounted sections were fixed in 4% paraformaldehyde for 10 min, washed three times in 0.1 M PBS, incubated in 1% hydrogen peroxide in 0.1 M PBS for 20 min, incubated twice in a 0.05% acetic anhydride solution, and blocked in 3% normal goat serum in 0.1 M PBS for 30 min prior to an overnight incubation in the anti-neuron-specific enolase antisera (1 : 500; Chemicon International). Sections were then incubated for 2 h with biotinylated secondary antisera (1 : 500; anti-rabbit raised in goat) in 3% normal goat serum in 0.1 M PBS. Sections were then washed three times in PBS and incubated for 1 h in avidin–biotin–peroxidase complex (Vector Laboratories). Peroxidase activity was labelled for 10 min with a 3,3-diaminobenzidine kit (Vector Laboratories).

Image acquisition and processing

Digital images of stained sections were captured with a DAGE-MTI cooled colour CCD camera and a Scion Series 7.0 three-chip frame grabber. Adobe Photoshop™ 5.0 for the Macintosh was used for image processing.

Patients and subjects

Nine adult or adolescent males with FXS [mean chronological age (CA) = 20.3 ± 9.5 years; mean verbal mental age (MA) = 9.1 ± 2.2 years] were recruited, and all had a DNA-confirmed diagnosis of FXS. Age- (CA = 20.4 ± 7.3) and IQ-matched male control subjects (CA 10.1 ± 2.6 years, MA = 10.5 ± 2.9 years) were recruited through a newspaper advertisement. Patients or their caregivers gave their or their ward's/child's written consent to take part in this study and were paid for their participation. The ethics committees of the Department of Psychology, McGill University, the Montreal Neurological Hospital and Institute and the Montreal Children's Hospital approved the study.

Cognitive assessment

IQ-matched controls were matched to the FXS patients on their overall mean performance on a test of verbal mental ability, as assessed by the Peabody Picture Vocabulary Test (PPVT-R, Form L; Dunn and Dunn, 1981) for English-speaking subjects or the Échelle de Vocabulaire en Images Peabody (EVIP, Forme A; Dunn *et al*., 1993) for French-speaking subjects. The PPVT and EVIP are individually administered tests that consist of 175 vocabulary items of increasing difficulty used to assess breadth of receptive language. A *t* test was performed to ensure that the group scores did not differ significantly ($t = 1.268$, $P = 0.11$).

Stimuli, procedure and apparatus

Spatial–temporal frequency contrast sensitivity

Test Gaussian enveloped sinusoidal wave gratings were generated with Morphonome® software (Smith-Kettlewell Eye Research Institute, San Francisco, CA) on a Macintosh computer fitted with a 21 inch CRT monitor, previously calibrated with the LightMouse® calibrator (Smith-Kettlewell Eye Research Institute) to ensure linear output at all luminance levels. The test gratings were orientated vertically and were reversed in contrast using a square wave temporal modulation profile. Contrast sensitivity measures were made with test gratings of 0.3 and 10.0 cycles/°, temporally modulated at either 1.2 or 18.8 Hz. The mean luminance of the patch was 31.1 cd/m^2 and subtended a diameter of 8° visual angle at 130 cm viewing distance. The patch was presented within a black cardboard surround with a circular aperture. During initial stimulus presentation, the luminance was counterphase modulated by 12% Michelson contrast and then increased or decreased according to a Yes/No one-up/two-down staircase procedure. Sufficient practice with near 100% contrast stimuli was allotted to all participants to ensure full comprehension of the task. The experimenter entered all responses. Catch trials with no stimulus presented were used to control for spurious responding. The staircase was terminated when the slope and SD of the last 12 trials was less than the step size. Detection thresholds were calculated as the mean value of the last 12 reversals. Eight FXS patients, 16 age-matched controls and eight IQ-matched controls performed this task.

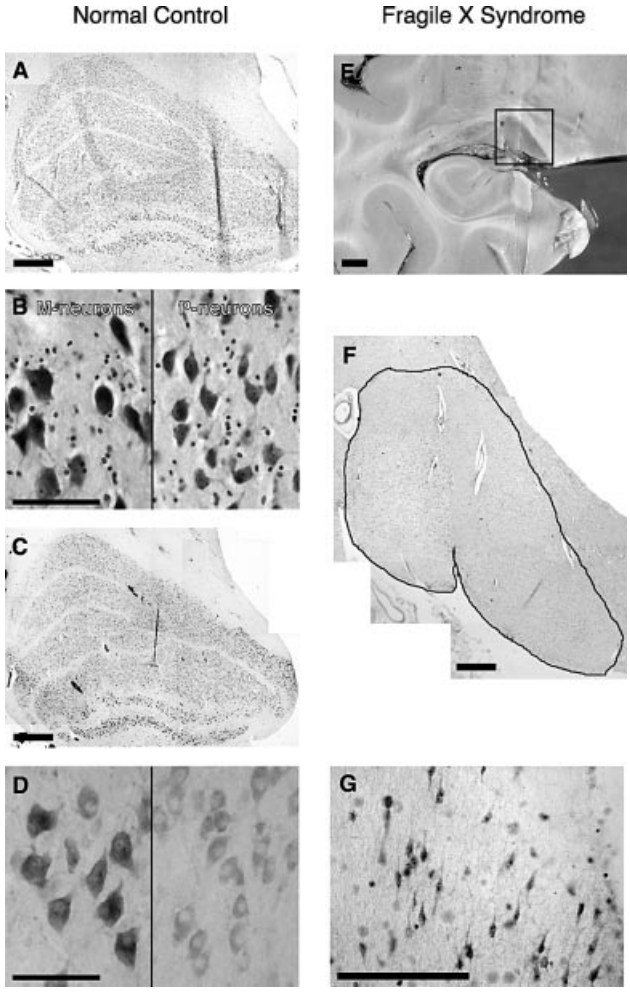

Fig. 1 FMRP immunoreactivity and Nissl staining in the LGN of a normal control and an FXS patient. (**A**) Composite image of the normal control LGN showing the characteristic six-layered structure; scale bar = 1000 μm. (**B**) High magnification images of Nissl-stained M and P neurons in the normal control LGN showing equal intensity of staining in both cell subtypes; scale bar = 100 μm. (**C**) Composite image of the normal control LGN showing the differential staining pattern for FMRP across the M and P layers; scale bar = 1000 μm. (**D**) High magnification images of FMRP staining of M and P neurons in the normal control LGN showing the greater immunoreactivity in the M neurons; scale bar = 100 μm. (**E**) Photograph of the left hemisphere from an FXS patient showing the location of the LGN used for subsequent immunohistochemical and histological processing; scale bar = 1000 μm. (**F**) Composite image of the FXS patient's LGN showing the abnormal alaminar structure; scale bar = 1000 μm. (**G**) High magnification image of Nissl-stained LGN cells from the FXS patient; scale bar = 100 μm.

Chromatic contrast sensitivity

Stimuli were red–green and blue–yellow Gaussian enveloped vertically oriented sinusoidal gratings (1 cycle/°, $\sigma = 2°$, displayed in a temporal Gaussian envelope, $\sigma = 125$ ms), presented on a 21 inch Sony Trinitron monitor (GDM-F500R) driven by a VSG (2/4) graphics board (Cambridge Research Systems Ltd, Rochester, UK) with 15 bits of contrast resolution, housed in a Pentium PC computer. The three stimuli were selected to isolate the two cone opponent (red–green and blue–yellow) post-receptoral mechanisms. The chromaticity of the stimuli was defined using a three-dimensional cone contrast space in which each axis represents the quantal catch of the L, M and S cone types normalized with respect to the white background (Mullen and Kingdom, 2002). Stimulus chromaticity and contrast are given by vector direction and magnitude, respectively, within the cone contrast space. Subjects were seated at a viewing distance of 57 cm from the stimuli. A method of adjustment was used in a Yes/No procedure to determine contrast threshold, which was calculated as the mean of three adjusted threshold values for each condition. The experimenter entered all responses. Four FXS patients, five age-matched controls and five IQ-matched controls performed this task.

Coherent motion

Motion stimuli were displayed on a Pentium PC computer fitted with a 15 inch monitor with subjects seated at a distance of ~50 cm. Detection of coherent motion was assessed using stimuli comprised of two ~15° × 25° random dot kinematograms (high luminance white dots on a black background, density 4 dots/$^{\circ 2}$), one of which was segregated into three horizontal strips, such that the direction of the coherent motion of the middle target strip was opposite to that of the two outer strips (as described in Wattam-Bell, 1996). The kinematogram on the opposite side of the screen displayed a uniform direction of coherent motion consistent with the direction of the two outer strips. During trials, a variable proportion of the dots oscillated horizontally across each array forming the coherent motion (velocity 6°/s), while the remaining dots moved in random directions. The direction of coherent motion reversed every 240 ms. Participants could not use a tracking strategy because the lifetime of each dot was limited to six video frames (70 ms). The additional 'noise' created by the disappearance of signal dots at the end of their lifetime was taken into account when calculating coherence levels on this task. Coherence level was varied according to a two-up/one-down staircase procedure starting with 100% coherent motion in the target strip. Sufficient practice with stimuli at 100% coherence was allotted to all participants to ensure full comprehension of the task. The experimenter entered all responses. Catch trials with 100% coherent motion were randomly interleaved into the experimental session to control for spurious responding. Participants were required to indicate the side (left or right) with the target strip exhibiting coherent motion. Coherence thresholds were calculated as the mean value of the last 10 reversals. Eight FXS patients, 16 age-matched controls and eight IQ-matched controls performed this task.

Coherent form

Form stimuli were displayed on a Pentium PC computer fitted with a 15 inch monitor with participants seated at a distance of ~50 cm. The form stimuli were composed of a static array of randomly orientated short line segments (white lines on a black background, density 1.3 segments/°) containing a target area on one side of the display where segments were oriented tangentially to form concentric circles (as described in Atkinson *et al*., 1997). The proportion of tangentially oriented line segments amongst the randomly oriented noise segments in the target area defined the coherence value for each trial. The coherence level was varied according to a two-up/one-down staircase procedure starting with 100% concentricity on the target side. Sufficient practice with stimuli at 100% concentricity was allotted to all participants to ensure full comprehension of the

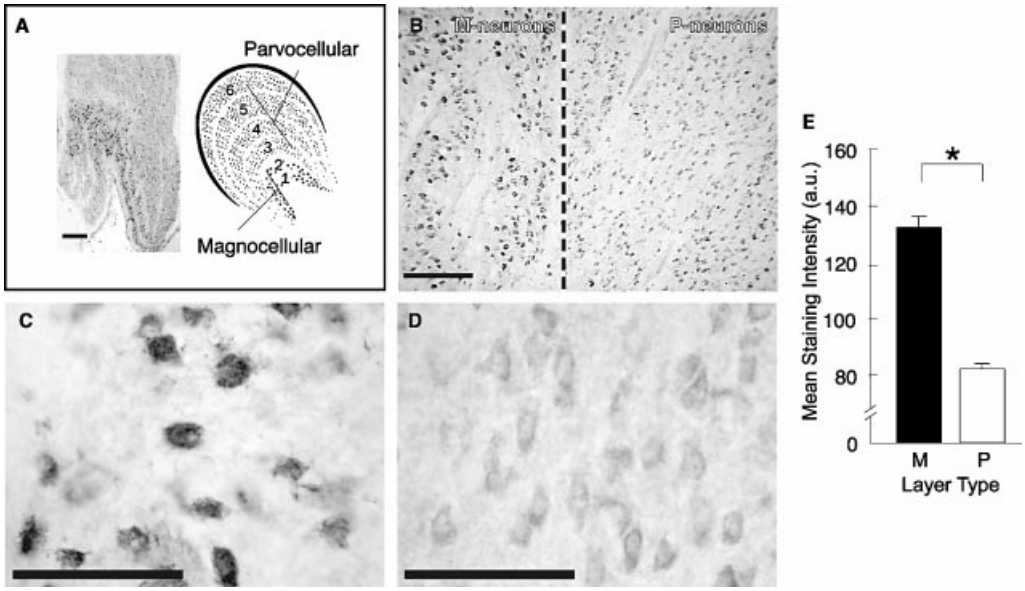

Fig. 2 FMRP immunoreactivity in monkey LGN. A differential staining pattern is apparent across the two parallel visual pathways at various magnifications, with M neurons showing greater immunostaining compared with P neurons. (**A**) Whole-LGN FMRP-stained image with adjacent schematic; scale bar = 1 mm. (**B**) Higher magnification image showing differential FMRP staining between M and P LGN layers; scale bar = 100 μm. Example images of (**C**) M and (**D**) P neurons used in quantitative analyses of FMRP expression level; scale bar = 25 μm. (**E**) Mean staining intensity for the two layer types in arbitrary units shows FMRP expression to be higher in M LGN neurons compared with their P LGN counterparts. Error bars represent ±1 SE; $*P < 0.0001$.

task. The experimenter entered all responses. Catch trials with 100% concentricity were randomly interleaved into the experimental session to control for spurious responding. Participants were asked to indicate the side (left or right) where the target strip exhibited coherent form. Coherence thresholds were calculated as the mean value of the last 10 reversals. Seven FXS patients, 16 age-matched controls and eight IQ-matched controls performed this task.

Results

Histology

We performed histological and immunohistochemical staining of both normal and FXS human LGN to determine the pattern of FMRP distribution in the M and P layers including possible neuroanatomical differences (Fig. 1). Nissl staining of the normal LGN revealed the characteristic six-layered structure with expected equal intensity of Nissl staining across the M and P neuron subtypes (Fig. 1A and B). The immunohistochemical results, on the other hand, showed clear differential staining, with a greater immunopositive reaction against the FMRP antigen in the M layers (layers 1 and 2) when compared with their P layer counterparts (layers 3–6; Fig. 1C and D). Unlike the normal control brain, both LGNs obtained from the FXS patient revealed an atypical structure (Fig. 1E) composed entirely of small sized neurons as revealed by Nissl staining (Fig. 1E and G). As expected, immunoreactivity to the anti-FMRP antibody was absent (data not shown).

To confirm and quantify the observed pattern of differential expression of FMRP across the M and P layers, we performed immunohistochemical staining of two monkey LGNs (Fig. 2). The results showed a staining pattern that was similar to that in the human LGN, with a greater immunopositive reaction in the M layers (Fig. 2A and B). This result was found to be quantitatively independent of known differences in the sizes of neurons comprising the two pathways. Intracellular differences were evaluated by comparing the mean staining intensity of identical marquees overlaid on high magnification images of a random sample of M and P LGN neurons (e.g. Fig. 2C and D). An ANOVA (analysis of variance) revealed a significant main effect of layer type, with M layer neurons having a significantly greater overall staining intensity [$F(1,21) = 97.44$, $P < 0.01$; Fig. 2E]. To verify the specificity of this result, we performed immunohistochemical analysis of adjacent sections for neuron-specific enolase, a protein known to be homogeneously distributed in the brain (Iwanaga *et al*., 1989). We found no significant differences in staining intensities across the geniculate layers for this antigen (data not shown). These results provide quantitative evidence that the expression level of FMRP is higher in M neurons than in P neurons, suggesting that the loss of FMRP in FXS may have a selective and detrimental impact on M pathway function in early vision.

Psychophysics

Spatial–temporal contrast sensitivity

To determine whether abnormal LGN morphology in FXS patients is associated with functional impairments, we compared contrast sensitivity measures for tasks that probe the M pathway in affected individuals with those from

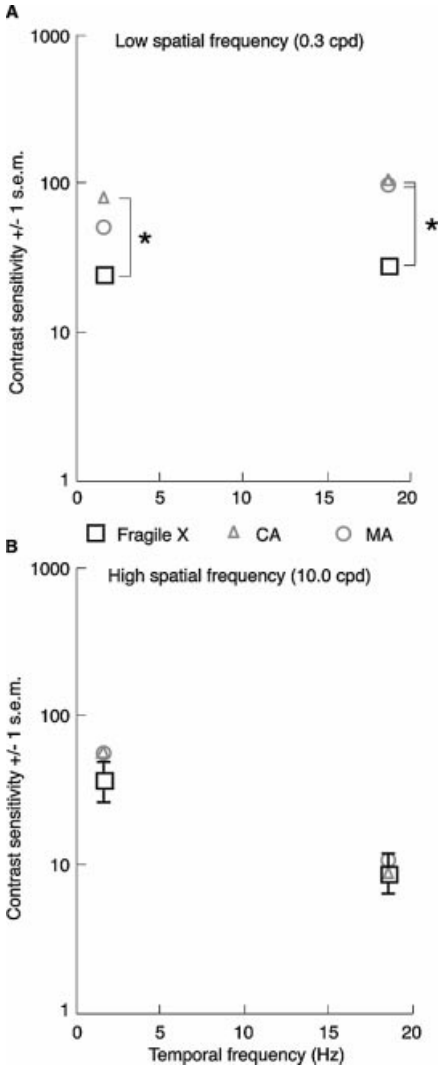

Fig. 3 Patients with FXS show a selective reduction in sensitivity for stimuli that preferentially engage the M pathway. (**A**) A significant loss in contrast sensitivity is seen in the FXS group (open squares) compared with the CA group (open triangles) for low spatial frequency [0.3 cycles/°(cpd)] gratings modulated at low temporal frequency (1.2 Hz). Similarly, a significant reduction in contrast sensitivity is apparent for the FXS group compared with both CA and MA (open circles) controls with low spatial frequency gratings modulated at high temporal frequency (18.8 Hz). (**B**) There is no decrement in contrast sensitivity among the three groups for high spatial frequency gratings modulated at either low or high temporal frequency. SE bars are omitted when smaller than the data point; *a significant difference based on *post hoc* Scheffé tests ($P << 0.0001$).

subjects matched by either CA or MA. Lesion (Merigan and Maunsell, 1990; Merigan *et al*., 1991; Lynch *et al*., 1992) and electrophysiological studies (Derrington and Lennie, 1984) in monkeys, as well as human (Tolhurst, 1975) psychophysical experiments have confirmed that the M and P pathways are sensitive to different types of stimuli. These studies showed that the M pathway is more sensitive to low spatial frequency sinusoidal gratings, particularly if modulated at higher temporal frequencies. In contrast, the P pathway is more sensitive to static higher spatial frequency sinusoidal gratings and chromatic stimuli. An ANOVA with group (FXS, CA and MA) as the independent measures variable and with temporal frequency (1.2 and 18.8 Hz) and spatial frequency (0.3 and 10.0 cycles/°) as the repeated measures variables revealed a significant three-way interaction [$F(2,29) = 3.557$, $P < 0.05$; Fig. 3]. *Post hoc* Scheffé tests confirmed that the FXS group had a significant reduction in contrast sensitivity for low spatial frequency stimuli modulated at both low and high temporal frequency when compared with the CA group. Comparison of the FXS group with the MA group also revealed a significant difference, but only for low spatial frequency stimuli modulated at high temporal frequency (Fig. 3A). In contrast, there were no significant differences among the three groups for high spatial frequency sine-wave gratings regardless of the temporal frequency at which they were modulated (Fig. 3B).

We also calculated the mean percentage loss in sensitivity for each condition where significant differences were found. The largest mean loss in sensitivity was evident in the FXS group for high temporal, low spatial frequency stimuli (mean loss = 73% compared with the CA group; 71% compared with the MA group). The next largest mean loss in sensitivity was found for low temporal, low spatial frequency stimuli (69%; compared with the CA group). These values are consistent with reported data from monkeys with experimentally induced M pathway lesions in the LGN (Merigan and Maunsell, 1990).

Although the stimuli we employed varied in spatial–temporal characteristics in order to engage the M or the P pathway selectively, it is possible that the observed deficits actually reflect a combined M and P pathway deficit resulting from some overlap in contrast sensitivity functions for the M and P pathways. To explore this possibility, we sought to test a perceptual function that is solely attributable to P pathway processing. We therefore took advantage of the fact that P neurons, but not M neurons, process the chromatic aspect of visual stimuli.

Chromatic contrast sensitivity

We assessed colour processing by measuring chromatic contrast thresholds for cardinal red–green and blue–yellow stimuli designed, respectively, to isolate the two subcortical cone opponent processes (Mullen and Kingdom, 2002). Neurons in the P pathway of primates are known to mediate colour vision, whereas those within the M pathway are functionally achromatic (Derrington *et al*., 1984; Merigan *et al*., 1991). An ANOVA with group (FXS, CA and MA) as the independent measures variable, and with chromatic pathway (blue–yellow and red–green) as the repeated measures variable, revealed a significant main effect of group [$F(2,11) = 4.366$, $P < 0.05$]. *Post hoc* Scheffé tests confirmed that there were no significant differences in colour contrast thresholds between the FXS group and the MA control group

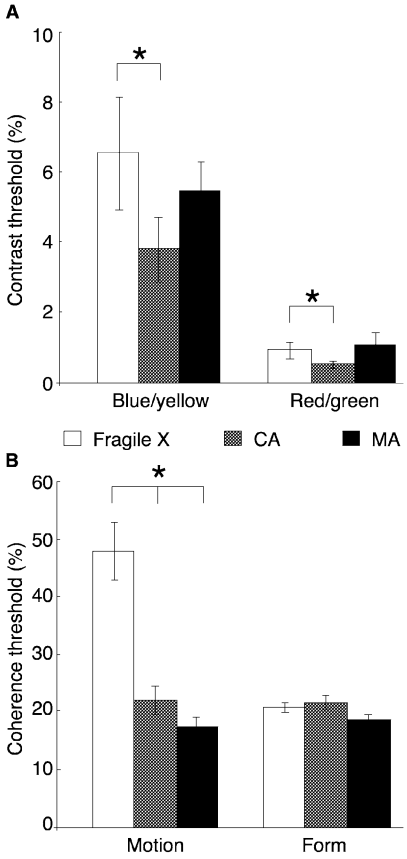

Fig. 4 Performance of FXS, CA and MA groups on tasks that probe colour, motion and form-processing mechanisms. (**A**) There is no significant difference in colour contrast thresholds between the FXS and MA groups for both blue–yellow and red–green gratings. However, the FXS group showed overall increased thresholds compared with the CA group. (**B**) A significant increase in motion coherence threshold was found for the FXS group compared with CA and MA controls. However, there was no decrement in form coherence threshold for the FXS group. Error bars represent ±1 SE; *a significant difference based on *post hoc* Scheffé tests (**A**, $P < 0.05$; **B**, $P < 0.001$).

(Fig. 4A). The finding that the CA control group had significantly lower colour contrast thresholds than both the FXS and MA groups indicates a mental age-dependent difference in the ability to perform the method of adjustment threshold task, and underscores the need for the MA control group.

The combined achromatic and chromatic psychophysical data suggest that loss of FMRP in FXS has a selective and detrimental impact on M pathway functioning without any measurable effects on P pathway functioning. We therefore sought to assess what affect, if any, the thalamic deficit may have on higher cortical processing. Although the cortical visual areas receive a mixture of inputs from M and P pathways, the DS is largely reliant on M pathway input and therefore is most vulnerable to disruptions in M pathway processing. To test this conjecture, we employed psychophysical tasks known to engage DS (parietal) and VS (temporal) processing, respectively.

Motion and form coherence

We expected that the M pathway impairments as well as the neuroanatomical abnormalities we observed in FXS patients would result in functional impairments of brain areas reliant on input from the LGN, namely the DS. Therefore, we tested our FXS patients and two control groups on a motion and a form coherence task that have been used recently to probe DS and VS function, respectively (Hansen *et al*., 2001; Gunn *et al*., 2002). An ANOVA with group (FXS, CA and MA) as the independent measure and task type (motion and form) as the repeated measure revealed a significant two-way interaction [$F(2,28) = 27.07$, $P < 0.01$]. *Post hoc* Scheffé tests confirmed that the FXS group had significantly elevated thresholds for the motion coherence task compared with both the CA and MA groups (Fig. 4B). Consistent with the spatial–temporal results that probed earlier stages of visual processing, FXS patients performed poorly on a global motion task when compared with both the MA and CA control groups, indicating a DS deficit in FXS. Conversely, there were no differences among the groups for the form coherence task, indicating a sparing of VS processing in FXS.

Discussion

Overall results

We have shown that FMRP expression is greater in M neurons in normal human LGN when compared with their P neuron counterparts. This difference was replicated and quantified in monkey LGN. We also provide evidence for cytoarchitectural changes in the LGN following the loss of FMRP in FXS. Specifically, neurons of the LGN of an FXS patient do not display the expected six-layered laminar structure. Rather, these cells appear as a homogenous population of small sized neurons when stained for Nissl substance. We have shown further that the neurobiological differences attributed to M neurons have a functional consequence for FXS patients. In particular, these individuals as a group, when compared with age- and IQ-matched controls, have raised thresholds for the detection of psychophysical stimuli that are processed preferentially by the M pathway. Importantly, we show that the deficit is not accounted for by a generalized perceptual impairment. In fact, the FXS group demonstrated performance equivalent to the control groups for the detection of psychophysical stimuli that are processed preferentially in the P pathway. Therefore, elevations in contrast threshold were most pronounced for high temporal and low spatial frequencies, with preserved thresholds for high spatial frequencies at all temporal frequencies tested. FXS patients were also able to perform as well as IQ-matched individuals on a test of chromatic sensitivity, an attribute unique to P neuron processing. Finally, FXS patients, when compared with age- and IQ-matched controls, showed perceptual deficits on a coherent motion task that recruits DS processing. No such deficit was found on an equivalent VS task of form coherence. The

present study therefore provides convergent histological and psychophysical data in support of an M neuron and DS deficit in FXS.

M neuron susceptibility?

Neurons comprising the M pathway respond preferentially to moving stimuli that inherently require fast neural processing for veridical transmission (Derrington and Lennie, 1984). M neurons are larger than P neurons, imparting them with the physiological advantage of being able to depolarize and repolarize rapidly, ideal for transmitting high temporal information. Furthermore, anatomical studies have shown that M pathway neurons maintain extensive dendritic fields that are significantly larger than those of the P pathway (Dacey and Petersen, 1992). The larger M neuron dendritic fields are believed to be necessary for integrating information across greater extents of visual space and allow for effective assimilation of dynamic stimuli, and therefore may be particularly susceptible to the loss of FMRP. Neurons of the P pathway, on the other hand, extract and convey information pertaining to stimulus form (Derrington and Lennie, 1984) and colour (Derrington *et al*., 1984). Unlike M neurons, P neurons are smaller in size and therefore are less suited to transmitting high temporal information. Furthermore, P neurons have smaller dendritic fields, reflecting their smaller receptive field sizes and, in turn, their greater suitability for transmitting high resolution detailed information critical for the identification of objects and for visual awareness.

The finding of cytoarchitectural changes in the LGN is consistent with a recent MRI study of FXS children and adolescents that found volumetric abnormalities in subcortical structures including the thalamus (Eliez *et al*., 2001). However, rather than suggesting a generalized thalamic abnormality, our neurobiological and neuroanatomical results show specifically that M neurons have a higher basal expression of FMRP. Furthermore, the LGNs from a FXS patient were composed of a homogenous population of small sized neurons rather than the expected mixed population of large (M) and small (P) neurons organized in their respective laminae. These findings support our hypothesis that *FMR1* is expressed in neurons of the M pathway but not the P pathway. Because cell size is a known physiological determinant of the capacity of a neuron to process high temporal frequency information (Derrington and Lennie, 1984), we postulate that the small sized LGN neurons that result from the lack of FMRP are therefore less efficient at, and perhaps, unsuited to encoding the type of information normally attributable to M neuron function.

Support for our hypothesis comes from a variety of studies, including those describing abnormalities in dendritic spine formation and pruning in the absence of FMRP, both in a knock-out mouse model of FXS and in post-mortem brains from FXS patients (Comery *et al*., 1997; Irwin *et al*., 2000, 2001, 2002; Greenough *et al*., 2001; Churchill *et al*., 2002). These studies reveal that in the absence of FMRP, neurons in the cortex have immature dendritic spines and are morphologically similar to those found in neurons from animals deprived of sensory experience. Furthermore, in FXS patients, the density of these immature spines was elevated when compared with normal control brains, suggesting a lack of appropriate synaptic elimination. The M and P neurons of the LGN of the thalamus differ in the sizes of their dendritic fields, reflecting their differential reliance on integration of information across areas of the visual field (Dacey and Petersen, 1992). M neurons may therefore be more susceptible to alterations in dendrite formation and maturation in the absence of FMRP because they rely on the convergence of information assimilated through their relatively larger dendritic fields.

Behavioural data and relevance to visual-motor impairments in FXS

We reasoned that the neurobiological impact of the lack of FMRP results in functional deficits of M pathway processing, thus providing a clear association between genetic changes, structural anomalies and behavioural deficits in FXS. The psychophysical measures employed in the present study were chosen to engage selectively either M or P pathway processing on the basis of prior electrophysiological (Derrington and Lennie, 1984) and psychophysical studies in monkeys (reviewed in Skottun, 2000) and humans (Tolhurst, 1975). It is critical in making claims for a selective deficit in perception to test other aspects of the given perceptual modality to ensure the specificity of the impairment. Therefore, in addition to employing detection tasks for stimuli that vary in spatial–temporal characteristics in order to recruit M pathway processing preferentially, we also tested spatial, temporal and chromatic processing in the P pathway of FXS patients. We further speculated that an M pathway deficit would have consequences for those cortical visual pathways that rely on its afferent input. In the case of the M pathway, there is a dominant projection to the DS of the parietal lobe (Ungerleider and Mishkin, 1982).

The FXS patients demonstrated the greatest reduction in sensitivity for low spatial frequency gratings modulated at high temporal frequency. However, these same patients had normal sensitivities for high spatial frequency gratings whether modulated at low or high temporal frequencies. These deficits are fully consistent with functional losses predicted from known spatial–temporal properties of the two subcortical visual pathways. Furthermore, the FXS group does not differ from the MA group for sensitivities to chromatic stimuli, confirming that the M pathway deficits are accompanied by a true sparing of P pathway function. In addition to highlighting the differential impact of the loss of FMRP on visual functioning in FXS, the fact that the FXS patients attained near normal performance for P pathway stimuli indicates that these individuals understood the tasks and could perform them as well as unaffected individuals.

Cortical visual functioning was assessed with form and motion coherence tasks that are thought to provide equivalent psychophysical measures of the general processing integrity of the VS and DS, respectively (Atkinson *et al*., 1997; Spencer *et al*., 2000; Gunn *et al*., 2002; O'Brien *et al*., 2002). These tasks require participants to integrate local form and motion elements to obtain a global understanding of the structure made up by these local elements. The ability of a given stream to extract global structure is thought to be fully encapsulated within a given stream and therefore not reliant on a domain-general integration system. As such, thresholds are thought to reflect the state of each stream accurately.

FXS patients were found to have increased thresholds for the detection of coherent motion in an array of randomly moving dots. Stimuli of this sort preferentially activate the medial temporal areas in monkeys (Newsome and Pare, 1988) and in humans (Tootell *et al*., 1995). Although it is possible that there are selective changes to the neurons of medial temporal areas and the parietal lobe due to the lack of FMRP that result in the observed motion coherence deficits, we believe that the most parsimonious explanation is that the M pathway deficits result in abnormal development of the DS. In other words, inadequate M pathway input to developing neural circuits of the DS during a critical period for development leads to impairments in parietal lobe function. In fact, immunohistochemical staining of a subset of brain areas associated with either the DS (e.g. medial temporal areas) or VS (e.g. V4) did not yield differential staining patterns such as those observed in the LGN (data not shown). The specificity of the functional impairment to the DS is supported further by the finding that FXS patients had similar thresholds for detection of global form signals.

A number of studies have described that FXS patients have impaired performance on neuropsychological tasks that assess visual-motor function (Crowe and Hay, 1990; Freund and Reiss, 1991; Maes *et al*., 1994; Cornish *et al*., 1999). However, the locus of the visual-motor impairment has not yet been identified. In the context of a model of the visual system proposed by Milner and Goodale (1995), visual control of action is mediated by the DS. Therefore, performance on motor-free tasks that probe the DS shed light on a potential perceptual deficit that will have an impact on visual-motor ability. We postulate that the difficulties that FXS individuals show in processing motion signals in the visual scene probably contribute to the observed visual-motor deficits. For example, the observed poor performance on a variety of drawing tasks (Crowe and Hay, 1990; Freund and Reiss, 1991) may reflect slow updating of motion signals to the DS due to the M pathway deficit, which may, in turn, lead to errors in visual guidance of hand movements. Similar impairments, termed constructional apraxia, have been described in patients with focal parietal lobe lesions (Villa *et al*., 1986). Likewise, all visually guided action requiring the manipulation of objects is likely to suffer. This may explain why FXS patients perform poorly on a variety of neuropsychological tasks that have a visual-motor component.

While this still leaves open the possibility that FXS patients also maintain difficulties in effectuating adaptive motor patterns, it is clear that without proper visual information processing at the input level, efferent signals will be compromised.

Relationship to other conditions

Motion perception deficits resulting from abnormal M neuron or DS function have been described previously in schizophrenia (Chen *et al*., 1999), Williams' syndrome (Atkinson *et al*., 1997), dyslexia (Livingstone *et al*., 1991) and autism (Spencer *et al*., 2000). The neurobiological basis of these conditions is probably the result of the synergistic effect of several genes, making it difficult to ascribe a single gene to the given phenotype. In contrast and by virtue of its single gene aetiology, FXS represents a unique model for understanding the impact of the *FMR1* gene on brain development and function.

It has been suggested that the DS is specifically vulnerable to atypical development (Atkinson, 2000), thereby leading to a preponderance of DS deficits in developmental disorders (Atkinson *et al*., 1997; Spencer *et al*., 2000; Gunn *et al*., 2002). In light of our findings, it is possible that the common cause of a DS deficit in this wide range of disorders is abnormal expression of FMRP or of other downstream or upstream modifiers of FMRP production.

Conclusion

The present study contributes to our understanding of the cognitive phenotype of FXS by showing that the M pathway and DS processing are impaired in FXS individuals, and by demonstrating the likely neurobiological substrate for such impairments. This study represents the first to show the impact of FMRP on visual processes and adds to and extends emerging work demonstrating the role of FMRP on early brain development.

The behavioural data presented here were limited to male FXS participants. Future investigations should include female FXS patients where a correlation between performance on the psychophysical tasks and the amount of FMRP expressed can be made. Such protein dosage effects have been demonstrated previously to be related to brain activation during arithmetic processing (Rivera *et al*., 2002) and working memory tasks (Menon *et al*., 2000; Kwon *et al*., 2001). It is interesting to note that Kwon *et al*. (2001) found a positive correlation between the amount of FMRP expressed and parietal lobe activation. Given that the majority of the DS is comprised of parietal lobe structures, the study of Kwon *et al*. (2001) strengthens the notion presented here of a relationship between FMRP expression and DS function. Future studies will probably clarify the link between lack of FMRP expression and abnormal brain morphology, leading to

further insights on the specific neurobiological and developmental determinants of the cognitive FXS phenotype.

Acknowledgements

We wish to thank C. Tyler for development and support of the psychophysical methodology, O. Braddick and J. Wattam-Bell for sharing the motion and form coherence programs, J. Desbarats for use of her microscope, and the participants and their families for volunteering their time. This work was supported by research grants from the Canadian Institutes of Health Research (CIHR) to A.C.

References

Atkinson J. The developing visual brain. Oxford: Oxford University Press; 2000.

Atkinson J, King J, Braddick O, Nokes L, Anker S, Braddick F. A specific deficit of dorsal stream function in Williams' syndrome. Neuroreport 1997; 8: 1919–22.

Belser RC, Sudhalter V. Conversational characteristics of children with fragile X syndrome: repetitive speech. Am J Ment Retard 2001; 106: 28–38.

Chen Y, Nakayama K, Levy DL, Matthysse S, Holzman PS. Psychophysical isolation of a motion-processing deficit in schizophrenics and their relatives and its association with impaired smooth pursuit. Proc Natl Acad Sci USA 1999; 96: 4724–9.

Churchill JD, Grossman AW, Irwin SA, Galvez R, Klintsova AY, Weiler IJ, et al. A converging-methods approach to fragile X syndrome. Dev Psychobiol 2002; 40: 323–38.

Comery TA, Harris JB, Willems PJ, Oostra BA, Irwin SA, Weiler IJ, et al. Abnormal dendritic spines in fragile X knockout mice: maturation and pruning deficits. Proc Natl Acad Sci USA 1997; 94: 5401–4.

Cornish KM, Munir F, Cross G. The nature of the spatial deficit in young females with fragile-X syndrome: a neuropsychological and molecular perspective. Neuropsychologia 1998; 36: 1239–46.

Cornish KM, Munir F, Cross G. Spatial cognition in males with fragile-X syndrome: evidence for a neuropsychological phenotype. Cortex 1999; 35: 263–71.

Cornish KM, Munir F, Cross G. Differential impact of the FMR-1 full mutation on memory and attention functioning: a neuropsychological perspective. J Cogn Neurosci 2001; 13: 144–50.

Crowe SF, Hay DA. Neuropsychological dimensions of the fragile X syndrome: support for a non-dominant hemisphere dysfunction hypothesis. Neuropsychologia 1990; 28: 9–16.

Dacey DM, Petersen MR. Dendritic field size and morphology of midget and parasol ganglion cells of the human retina. Proc Natl Acad Sci USA 1992; 89: 9666–70.

Derrington AM, Lennie P. Spatial and temporal contrast sensitivities of neurones in lateral geniculate nucleus of macaque. J Physiol 1984; 357: 219–40.

Derrington AM, Krauskopf J, Lennie P. Chromatic mechanisms in lateral geniculate nucleus of macaque. J Physiol 1984; 357: 241–65.

Dunn LM, Dunn LM. Peabody picture vocabularly test-revised, American Guidance Service, Mininnesota 1981.

Dunn LM, Thériault CM, Dunn LM. Échelle de vocabulaire en images Peabody. American Guidence Service, Minnesota 1993.

Dykens EM, Hodapp RM, Ort S, Finucane B, Shapiro LR, Leckman JF. The trajectory of cognitive development in males with fragile X syndrome. J Am Acad Child Adolesc Psychiatry 1989; 28: 422–6.

Eliez S, Blasey CM, Freund LS, Hastie T, Reiss AL. Brain anatomy, gender and IQ in children and adolescents with fragile X syndrome. Brain 2001; 124: 1610–8.

Felleman DJ, Burkhalter A, Van Essen DC. Cortical connections of areas V3 and VP of macaque monkey extrastriate visual cortex. J Comp Neurol 1997; 379: 21–47.

Freund LS, Reiss AL. Cognitive profiles associated with the fra(X) syndrome in males and females. Am J Med Genet 1991; 38: 542–7.

Greenough WT, Klintsova AY, Irwin SA, Galvez R, Bates KE, Weiler IJ. Synaptic regulation of protein synthesis and the fragile X protein. Proc Natl Acad Sci USA 2001; 98: 7101–6.

Gunn A, Cory E, Atkinson J, Braddick O, Wattam-Bell J, Guzzetta A, et al. Dorsal and ventral stream sensitivity in normal development and hemiplegia. Neuroreport 2002; 13: 843–7.

Hagerman RJ. Fragile X syndrome. Curr Probl Pediatr 1987; 17: 621–74.

Hagerman RJ, Hagerman PJ. Fragile X syndrome: diagnosis, treatment and research. 3rd edn. Baltimore (MD): The Johns Hopkins University Press; 2002.

Hansen PC, Stein JF, Orde SR, Winter JL, Talcott JB. Are dyslexics' visual deficits limited to measures of dorsal stream function? Neuroreport 2001; 12: 1527–30.

Irwin SA, Galvez R, Greenough WT. Dendritic spine structural anomalies in fragile-X mental retardation syndrome. Cereb Cortex 2000; 10: 1038–44.

Irwin SA, Patel B, Idupulapati M, Harris JB, Crisostomo RA, Larsen BP, et al. Abnormal dendritic spine characteristics in the temporal and visual cortices of patients with fragile-X syndrome: a quantitative examination. Am J Med Genet 2001; 98: 161–7.

Irwin SA, Idupulapati M, Gilbert ME, Harris JB, Chakravarti AB, Rogers EJ, et al. Dendritic spine and dendritic field characteristics of layer V pyramidal neurons in the visual cortex of fragile-X knockout mice. Am J Med Genet 2002; 111: 140–6.

Iwanaga T, Takahashi Y, Fujita T. Immunohistochemistry of neuron-specific and glia-specific proteins. Arch Histol Cytol 1989; 52 Suppl: 13–24.

Jakala P, Hanninen T, Ryynanen M, Laakso M, Partanen K, Mannermaa A, et al. Fragile-X: neuropsychological test performance, CGG triplet repeat lengths, and hippocampal volumes. J Clin Invest 1997; 100: 331–8.

Kwon H, Menon V, Eliez S, Warsofsky IS, White CD, Dyer-Friedman J, et al. Functional neuroanatomy of visuospatial working memory in fragile X syndrome: relation to behavioral and molecular measures. Am J Psychiatry 2001; 158: 1040–51.

Le S, Cardebat D, Boulanouar K, Henaff MA, Michel F, Milner D, et al. Seeing, since childhood, without ventral stream: a behavioural study. Brain 2002; 125: 58–74.

Livingstone MS, Rosen GD, Drislane FW, Galaburda AM. Physiological and anatomical evidence for a magnocellular defect in developmental dyslexia. Proc Natl Acad Sci USA 1991; 88: 7943–7.

Lynch JJ 3rd, Silveira LC, Perry VH, Merigan WH. Visual effects of damage to P ganglion cells in macaques. Vis Neurosci 1992; 8: 575–83.

Maes B, Fryns JP, Van Walleghem M, Van den Berghe H. Cognitive functioning and information processing of adult mentally retarded men with fragile-X syndrome. Am J Med Genet 1994; 50: 190–200.

Menon V, Kwon H, Eliez S, Taylor AK, Reiss AL. Functional brain activation during cognition is related to FMR1 gene expression. Brain Res 2000; 877: 367–70.

Merigan WH, Maunsell JH. Macaque vision after magnocellular lateral geniculate lesions. Vis Neurosci 1990; 5: 347–52.

Merigan WH, Katz LM, Maunsell JH. The effects of parvocellular lateral geniculate lesions on the acuity and contrast sensitivity of macaque monkeys. J Neurosci 1991; 11: 994–1001.

Milner AD, Goodale MA. The visual brain in action. Oxford: Oxford University Press; 1995.

Mostofsky SH, Mazzocco MM, Aakalu G, Warsofsky IS, Denckla MB, Reiss AL. Decreased cerebellar posterior vermis size in fragile X syndrome: correlation with neurocognitive performance. Neurology 1998; 50: 121–30.

Mullen KT, Kingdom FA. Differential distributions of red–green and blue–yellow cone opponency across the visual field. Vis Neurosci 2002; 19: 109–18.

Munir F, Cornish KM, Wilding J. Nature of the working memory deficit in fragile-X syndrome. Brain Cogn 2000*a*; 44: 387–401.

Munir F, Cornish KM, Wilding J. A neuropsychological profile of attention

deficits in young males with fragile X syndrome. Neuropsychologia 2000*b*; 38: 1261–70.

Newsome WT, Pare EB. A selective impairment of motion perception following lesions of the middle temporal visual area (MT). J Neurosci 1988; 8: 2201–11.

O'Brien J, Spencer J, Atkinson J, Braddick O, Wattam-Bell J. Form and motion coherence processing in dyspraxia: evidence of a global spatial processing deficit. Neuroreport 2002; 13: 1399–402.

Oberle I, Rousseau F, Heitz D, Kretz C, Devys D, Hanauer A, et al. Instability of a 550-base pair DNA segment and abnormal methylation in fragile X syndrome. Science 1991; 252: 1097–102.

Pieretti M, Zhang FP, Fu YH, Warren ST, Oostra BA, Caskey CT, et al. Absence of expression of the FMR-1 gene in fragile X syndrome. Cell 1991; 66: 817–22.

Reiss AL, Freund L. Fragile X syndrome, DSM-III-R, and autism. J Am Acad Child Adolesc Psychiatry 1990; 29: 885–91.

Rivera SM, Menon V, White CD, Glaser B, Reiss AL. Functional brain activation during arithmetic processing in females with fragile X syndrome is related to FMR1 protein expression. Hum Brain Mapp 2002; 16: 206–18.

Schapiro MB, Murphy DG, Hagerman RJ, Azari NP, Alexander GE, Miezejeski CM, *et al*. Adult fragile X syndrome: neuropsychology, brain anatomy, and metabolism. Am J Med Genet 1995; 60: 480–93.

Skottun BC. The magnocellular deficit theory of dyslexia: the evidence from contrast sensitivity. Vision Res 2000; 40: 111–27.

Spencer J, O'Brien J, Riggs K, Braddick O, Atkinson J, Wattam-Bell J. Motion processing in autism: evidence for a dorsal stream deficiency. Neuroreport 2000; 11: 2765–7.

Tolhurst DJ. Sustained and transient channels in human vision. Vision Res 1975; 15: 1151–5.

Tootell RB, Reppas JB, Kwong KK, Malach R, Born RT, Brady TJ, et al. Functional analysis of human MT and related visual cortical areas using magnetic resonance imaging. J Neurosci 1995; 15: 3215–30.

Turk J. Fragile X syndrome and attentional deficits. J Appl Res Intellect Disabil 1998; 11: 175–191.

Turk J, Cornish K. Face recognition and emotion perception in boys with fragile-X syndrome. J Intellect Disabil Res 1998; 42: 490–9.

Turner G, Webb T, Wake S, Robinson H. Prevalence of fragile X syndrome. Am J Med Genet 1996; 64: 196–7.

Ungerleider LG, Mishkin M. Two cortical visual systems. In: Ingle DJ, Goodale MA, Mansfield RJW, editors. Analysis of visual behavior. Cambridge (MA): MIT Press; 1982. p. 549–86.

Verkerk AJ, Pieretti M, Sutcliffe JS, Fu YH, Kuhl DP, Pizzuti A, et al. Identification of a gene (FMR-1) containing a CGG repeat coincident with a breakpoint cluster region exhibiting length variation in fragile X syndrome. Cell 1991; 65: 905–14.

Vidyasagar TR. From attentional gating in macaque primary visual cortex to dyslexia in humans. Prog Brain Res 2001; 134: 297–312.

Villa G, Gainotti G, De Bonis C. Constructional disabilities in focal brain-damaged patients. Influence of hemispheric side, locus of lesion and coexistent mental deterioration. Neuropsychologia 1986; 24: 497–510

Wattam-Bell J. Visual motion processing in one-month-old infants: preferential looking experiments. Vision Res 1996; 36: 1671–7.

Wilding J, Cornish K, Munir F. Further delineation of the executive deficit in males with fragile-X syndrome. Neuropsychologia 2002; 40: 1343–9.